








Dissociation between neuroanatomical and symptomatic subtypes in schizophrenia

Chao Chai¹ , Hao Ding², Xiaotong Du¹ , Yingying Xie¹, Weiqi Man^{1,3}, Yu Zhang¹, Yi Ji¹ , Meng Liang² , Bin Zhang⁴ , Yuping Ning⁴, Chuanjun Zhuo⁵, Chunshui Yu^{1,2}  and Wen Qin¹ 

Research Article

Cite this article: Chai C, Ding H, Du X, Xie Y, Man W, Zhang Y, Ji Y, Liang M, Zhang B, Ning Y, Zhuo C, Yu C, Qin W (2023). Dissociation between neuroanatomical and symptomatic subtypes in schizophrenia. *European Psychiatry*, **66**(1), e78, 1–12
<https://doi.org/10.1192/j.eurpsy.2023.2446>

Received: 31 October 2022

Revised: 20 May 2023

Accepted: 01 August 2023

Keywords:

gray matter volume; heterogeneity; magnetic resonance imaging; Positive and Negative Syndrome Scale; schizophrenia; subtypes

Corresponding authors:

Wen Qin, Chunshui Yu, and Chuanjun Zhuo;

Emails: wayne.wenqin@gmail.com;

chunshuiyu@tmu.edu.cn;

chuanjunzhuo@tmu.edu.cn

C.C. and H.D. contributed equally to the work.

¹Department of Radiology and Tianjin Key Laboratory of Functional Imaging, Tianjin Medical University General Hospital, Tianjin, China; ²School of Medical Imaging, Tianjin Medical University, Tianjin, China; ³Academy of Medical Engineering and Translational Medicine, Tianjin University, Tianjin, China; ⁴Department of Psychiatry, Affiliated Brain Hospital of Guangzhou Medical University, Guangzhou, China and ⁵Department of Psychiatry, Tianjin Fourth Center Hospital, Tianjin, China

Abstract

Background. Schizophrenia is a complex and heterogeneous syndrome with high clinical and biological stratification. Identifying distinctive subtypes can improve diagnostic accuracy and help precise therapy. A key challenge for schizophrenia subtyping is understanding the subtype-specific biological underpinnings of clinical heterogeneity. This study aimed to investigate if the machine learning (ML)-based neuroanatomical and symptomatic subtypes of schizophrenia are associated.

Methods. A total of 314 schizophrenia patients and 257 healthy controls from four sites were recruited. Gray matter volume (GMV) and Positive and Negative Syndrome Scale (PANSS) scores were employed to recognize schizophrenia neuroanatomical and symptomatic subtypes using *K*-means and hierarchical methods, respectively.

Results. Patients with ML-based neuroanatomical subtype-1 had focally increased GMV, and subtype-2 had widespread reduced GMV than the healthy controls based on either *K*-means or Hierarchical methods. In contrast, patients with symptomatic subtype-1 had severe PANSS scores than subtype-2. No differences in PANSS scores were shown between the two neuroanatomical subtypes; similarly, no GMV differences were found between the two symptomatic subtypes. Cohen's Kappa test further demonstrated an apparent dissociation between the ML-based neuroanatomical and symptomatic subtypes ($P > 0.05$). The dissociation patterns were validated in four independent sites with diverse disease progressions (chronic vs. first episodes) and ancestors (Chinese vs. Western).

Conclusions. These findings revealed a replicable dissociation between ML-based neuroanatomical and symptomatic subtypes of schizophrenia, which provides a new viewpoint toward understanding the heterogeneity of schizophrenia.

Introduction

Schizophrenia is a complex, chronic, heterogeneous, and devastating psychotic syndrome that causes a considerable healthcare burden worldwide [1, 2]. Patients with schizophrenia have a reduced life expectancy of about 15 years compared with the general population [3, 4]. However, the diagnosis of schizophrenia is impacted by the heterogeneity in clinical presentation, biomarker expression, illness course, functional outcome, treatment response, and so on [5–11]. Identifying distinctive subtypes of schizophrenia can improve diagnostic accuracy and help precise therapy [12, 13].

Before the emergence of objective quantification such as neuroimaging and genetic measures, psychiatrists often categorized the subtypes of schizophrenia based on patients' clinical symptoms. For example, schizophrenia was traditionally classified into paranoid, catatonic, disorganized subtypes, and so forth, based on the Diagnostic and Statistical Manual of Mental Disorders (DSM) and International Classification of Diseases (ICD) classification systems [14]. Some scholars also tried to subdivide schizophrenia based on the symptom dimensions, such as the Positive and Negative Syndrome Scale (PANSS) [15–18], Assessment of Positive/Negative Symptoms [19, 20], or cognitive performance [21–23]. With the advance of big data mining and pattern recognition, unsupervised machine learning (ML) techniques are emerging to recognize the biological subtypes of various neuropsychiatric diseases [24]. Compared to traditional manual subtyping by clinicians according to diagnostic guidelines, unsupervised ML is a type of powerful data-driven technique designed to recognize the intrinsic stratified structure of unlabeled data, and thus is more objective and could reproducibly identify subtypes in neuropsychiatric diseases from high dimensional features that are difficult or impossible for humans to discriminate [25]. ML techniques have shown the potential to classify schizophrenia

© The Author(s), 2023. Published by Cambridge University Press on behalf of the European Psychiatric Association. This is an Open Access article, distributed under the terms of the Creative Commons Attribution-NonCommercial-ShareAlike licence (<http://creativecommons.org/licenses/by-nc-sa/4.0>), which permits non-commercial re-use, distribution, and reproduction in any medium, provided the same Creative Commons licence is used to distribute the re-used or adapted article and the original article is properly cited. The written permission of Cambridge University Press must be obtained prior to any commercial use.



EUROPEAN PSYCHIATRIC ASSOCIATION

patients into several subtypes with diverse symptomatic patterns [16, 17, 19, 20]. Besides, ML techniques have been recently applied to subtype schizophrenia based on the biological measures derived from magnetic resonance imaging (MRI), such as white matter microstructural measures from diffusion tensor imaging (DTI), and gray matter morphometric measures from structural MRI [5, 8, 12, 13, 22, 26–30]. These ML-based subtyping techniques might provide an objective way for a precise diagnosis of schizophrenia.

A key challenge for ML-based schizophrenia subtyping is its interpretability for psychiatrists. Bridging the gap between ML-based neuroimaging subtypes and clinical phenotypes could not only deepen the understanding of the biological underpinnings contributing to clinical heterogeneity, but also promote the application of the ML-based subtypes in disease diagnosis and treatments. For example, it has been shown that neuroanatomical subtyping could enhance discrimination of schizophrenia from the healthy controls [12]. However, there remains debate on the clinical symptomatic relevance of neuroanatomical subtypes derived from ML techniques, and vice versa for symptomatic subtypes. Although noticeable brain structural differences were reported among symptomatic subtypes based on ML techniques, most studies only reported subtle differences, no difference, or considerable overlap in brain signatures among subtypes, which impeded the interpretation of these ML-based clinical subtypes [16, 17, 19, 20]. Similar situations were also shown for ML-based neuroimaging subtypes. For example, no PANSS differences were reported between schizophrenia neuroimaging subtypes using gray matter volume (GMV) by several independent studies [5, 12, 13, 27, 31]. And only differences in negative symptoms were identified between neuroimaging subtypes derived from white matter DTI metrics [26].

In this study, we tried to elucidate the potential association between the ML-based neuroanatomical subtypes and symptomatic subtypes in schizophrenia patients, namely, whether the ML-based neuroanatomical subtypes had different clinical manifestations, or the ML-based symptomatic subtypes had different neuroanatomic damage patterns. It should be noted that early reported schizophrenia subtypes were significantly diverse across different studies in either a number of categories or manifestations, which may be induced by sample heterogeneities (such as medication history and disease progression) and subtyping methods diversity [5, 12, 17, 30]. Therefore, to account for these confounding factors, this study planned to enroll a relatively large schizophrenia sample from four independent sites, including the chronic and drug-naïve first-episode patients. Besides, we applied two publicly used ML methods that had been used for psychiatric diseases subtyping [26, 32], *K*-means and hierarchical clustering, to validate if the ML-based subtypes are stable by different algorithms. Specifically, we aimed to explore: (1) Brain GMV difference between PANSS-derived subtypes clustered using the *K*-means and hierarchical methods; (2) PANSS differences between two GMV-derived subtypes using the *K*-means and hierarchical methods; (3) the consistency and diversity between different subtyping

methods (*K*-means vs. hierarchical), and between different features (PANSS vs. GMV); and (4) the effects of sites on the subtyping classification.

Materials

Subjects

This study included two independent Chinese structural MRI (sMRI) datasets from Tianjin Medical University General Hospital (TIANJIN) (112 patients and 106 HCs) and Guangzhou Medical University affiliated Brain Hospital (GUANGZHOU) (51 patients and 29 HCs), and two Western public datasets from the SchizConnect database [33], including BrainGluSchi (71 patients and 44 HCs) [34] and COBRE (80 patients and 78 HCs) [34]. Patients from TIANJIN, BrainGluSchi, and COBRE were chronic and had stable antipsychotic medication. And patients from GUANGZHOU were drug-naïve and first-episode. All the patients with schizophrenia were diagnosed based on the structured clinical interview for DSM-IV axis I disorders (SCID-I). In addition, patients' psychopathology ratings were assessed using the PANSS at MRI examination. The nonpatient version of SCID was applied to ensure the lifetime absence of psychiatric illness in the HCs, and there were also no known histories of major psychiatric illness in HCs' first-degree relatives. The subjects were excluded if they had other neurological and psychiatric disorders, present or past regular alcohol and illicit drug abuse, a history of traumatic brain injury with consciousness loss, MRI contraindication, or electroconvulsive treatment. Finally, 314 schizophrenia patients (age range, 41–59; mean, 33.81 ± 11.03 ; male, 217; female, 97) and 257 healthy controls (HCs) (age range, 41–59; mean, 34.40 ± 10.91 ; male, 159; female, 98) were recruited. The local Ethics Committees approved the enrollment of TIANJIN and GUANGZHOU datasets, and the subjects from the corresponding institutes gave their informed written consent before the MRI scanning.

MRI data acquisition

MRI data of BrainGluSchi and COBRE sites were collected using the 3.0 T Siemens Trio Tim scanner (Siemens Healthineers, Erlangen, Germany). MRI data of the TIANJIN and GUANGZHOU sites were collected using the 3.0 T GE Discovery MR750 system (General Electric, Milwaukee, WI) and the 3.0 T Philips Achieva scanner (Philips, Andover, MA), respectively. The sMRI sequence parameters of each scanner are listed in Table 1.

Data preprocessing

The sMRI data underwent standard voxel-based morphometry (VBM) pipeline to derive the absolute GMV and smoothed with 8-mm full-width at half-maximum (FWHM) (Supplementary Methods: MRI Data Preprocessing). Next, Combat harmonization

Table 1. The parameters of 3D T1 sMRI data from different MRI scanners in each site

Sites	Device	Strength (Tesla)	TR (ms)	TE (ms)	T1 (ms)	FA (degree)	Matrix	Voxel size (mm)
BrainGluSchi	Siemens Trio	3.0 T	2530	1.64	1200	7	256 × 256 × 176	1.0 × 1.0 × 1.0
COBRE	Siemens Trio	3.0 T	2530	1.64	1200	7	256 × 256 × 176	1.0 × 1.0 × 1.0
TIANJIN	GE MR750	3.0 T	8.2	3.2	450	12	256 × 256 × 188	1.0 × 1.0 × 1.0
GUANGZHOU	Philips Achieva	3.0 T	8.2	3.7	1100	7	256 × 256 × 188	1.0 × 1.0 × 1.0

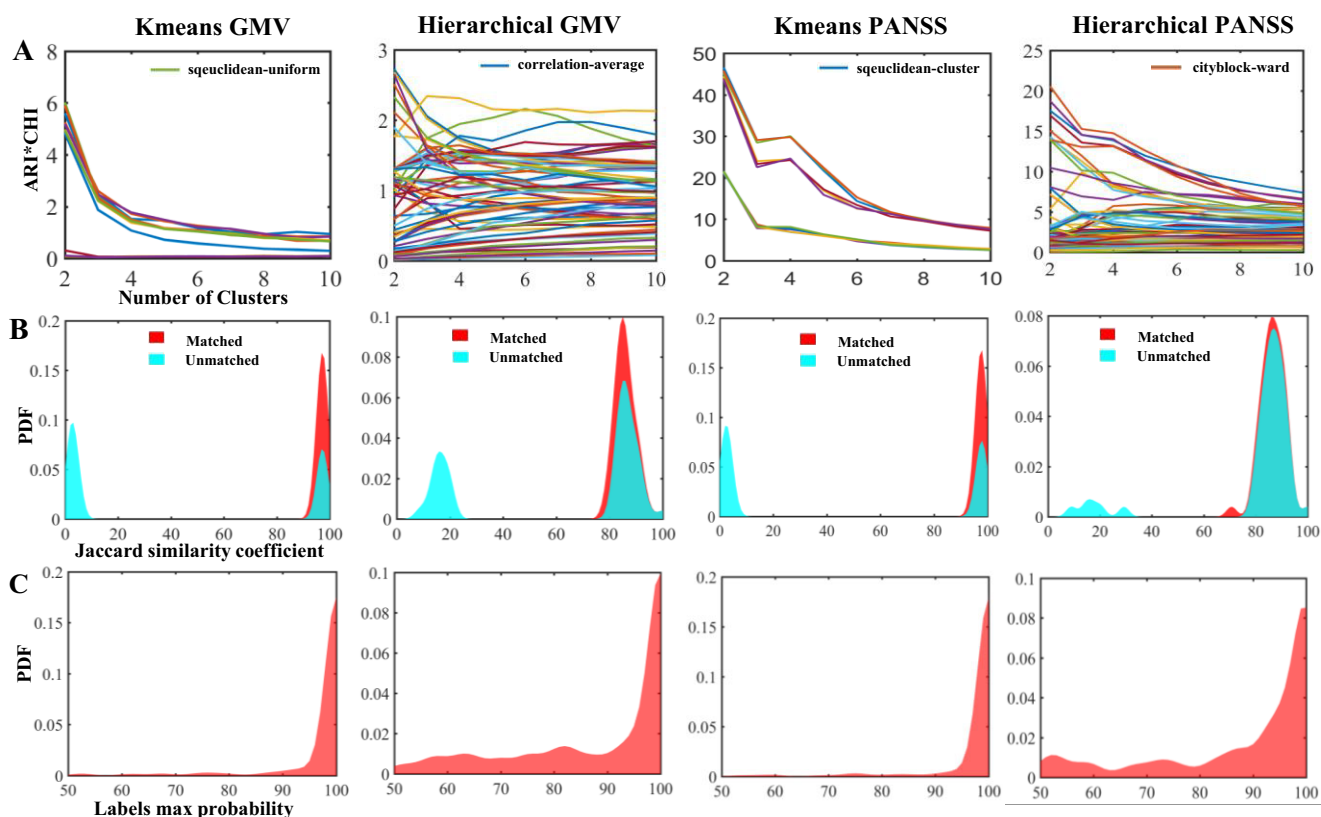


Figure 1. Subtyping performance evaluation. (A) The best model is based on ARI*CHI criteria during *K*-means and Hierarchical clustering in two (PANSS vs. GMV) feature types. (B) The Jaccard similarity coefficients between shuffles before (cyan) and after (red) labels match the best model. A larger coefficient represents a better match across shuffles. (C) The max probability of each patient across 50 shuffles. Max probability of most individuals was higher than 80%, indicating the reproducibility of subtyping.

was performed to eliminate the systematic bias in GMV and PANSS across four sites [35]. Then a linear regression was applied to regress out confounders for metrics (age, sex, and TIV for GMV; age and sex for PANSS). Finally, a principal component analysis (PCA) was carried out on unsmoothed GMV to extract the top 464 components that explain 95% variance for clustering analysis (Supplementary Methods: Data Harmonization and Feature Extraction).

Subtypes identification based on ML

K-means and Hierarchical clustering algorithms were used to cluster the recruited schizophrenia patients into different subtypes based on the GMV (464 features) and PANSS data (30 features), respectively. A 10 randomization 5-fold cross-validation strategy was used to estimate and eliminate sample selection bias during clustering. The multiplication of Calinski-Harabasz Index (CHI) and Adjusted Rand Index (ARI) was used to determine the best clustering hyperparameters for *K*-means and Hierarchical clustering methods. Finally, the Jaccard similarity coefficient was used to match the clustering labels across shuffles, and the label with the maximum probability across all shuffles was considered as the subtype ID of this subject (Supplementary Methods: Subtypes Identification).

Statistical analysis

Neuroimaging data analyses were performed using SPM12 software. The statistical analyses of tabular data were performed using SPSS software (version 17.0, SPSS Inc.).

One-way analysis of variance, the Mann-Whitney *U* test, Kappa test, two-sample *t*-test, Spearman correlation, and Kolmogorov-Smirnov test were performed in our study. The detailed descriptions of statistical methods were provided in Supplementary Methods: Statistical Analysis section.

Results

Clustering performance

As shown in Figure 1, both *K*-means and Hierarchical clustering methods identified two neuroanatomical subtypes (*K*-means: ARI*CHI = 6.018; Hierarchical: ARI*CHI = 2.724) and two symptomatic subtypes (*K*-means: ARI*CHI = 46.573; Hierarchical: ARI*CHI = 20.557) according to the chosen best model (Figure 1A). Jaccard similarity coefficients demonstrated high similarity between shuffles for the neuroanatomical subtypes using *K*-means (median = 0.974, interquartile range [IQR] = [0.964, 0.980]) and Hierarchical clustering (median = 0.855, IQR = [0.834, 0.885]), and for the symptomatic subtypes using *K*-means (median = 0.975, IQR = [0.970, 0.985]) and Hierarchical clustering (median = 0.864, IQR = [0.833, 0.897]), indicating high repeatability of the clustering across shuffles (Figure 1B). The maximum probability of the subtypes across shuffles was also high for neuroanatomical subtypes using *K*-means (median = 1.000, IQR = [1.000, 1.000]) and Hierarchical clustering (median = 0.985, IQR = [0.800, 1.000]), and for symptomatic subtypes using *K*-means (median = 1.000, IQR = [1.000, 1.000]) and Hierarchical clustering (median = 0.950, IQR = [0.825, 1.000]),

further supporting that the subtype for each subject was reliable across different randomizations (Figure 1C).

Demographics and clinical characteristics of subtypes

There were no significant differences in age, gender, and TIV among the neuroanatomical subtypes and HCs in the total cohort (Table 2) and in each site (Supplementary Tables 1–4) using either *K*-means and Hierarchical clustering (all $P > 0.05$). Neuroanatomical subtype-1 based on the *K*-means clustering method had significantly lower CPZ equivalents than subtype-2 in the total cohort ($z = -2.859, P = 0.004$) (Table 2) and in BrainGluSchi dataset ($z = -2.768, P = 0.006$) (Supplementary Table 1). In addition, neuroanatomical subtype-1 using Hierarchical clustering had lower CPZ equivalents ($z = -3.007, P = 0.003$), lower age when schizophrenia was first diagnosed ($z = -2.064, P = 0.039$), lower age when symptoms firstly appeared ($z = -1.998, P = 0.046$), and lower age when therapy was firstly received ($z = -2.994, P = 0.003$) than subtype-2 in the total cohort (Table 2). Neuroanatomical subtype-1 based on Hierarchical clustering had lower CPZ equivalents ($z = -2.224, P = 0.026$), lower age when therapy first received ($z = -2.077, P = 0.038$) than subtype-2 in COBRE dataset (Supplementary Table 2). There were no significant differences in clinical indicators among the symptomatic subtypes and HCs in either the total cohort or each site ($P > 0.05$) (Table 2 and Supplementary Tables 3 and 4).

GMV features of the GMV-derived subtypes

One-way ANOVA found neuroanatomical subtype-1 based on the *K*-means method had focally increased GMV in the left medial orbital superior frontal gyrus (moSFG), left superior frontal gyrus (SFG), bilateral middle frontal gyrus (MFG), and right supplementary motor area (SMA), and right precentral gyrus (PrecG) than the HCs; in contrast, neuroanatomical subtype-2 also had broadly reduced GMV than the HCs, especially in the bilateral orbital frontal lobes, thalamus, insular and medial prefrontal cortex (MPFC) (Figure 2A). The GMV changes patterns of the neuroanatomical subtypes using the Hierarchical method were similar to those using the *K*-means method (Figure 3A) ($P < 0.05$, voxel-wise FWE corrected).

The GMV of neuroanatomical subtype-2 was broadly lower than in subtype-1 using either *K*-means (Figure 2A) or the Hierarchical clustering method (Figure 3A) ($P < 0.05$, voxel-wise FWE corrected), which was replicated at each of the four sites (Figures 2B and 3B) ($P < 0.05$, cluster-wise FWE corrected). Further spatial correlation analyses demonstrated a significant positive association in *T*-distributions of inter-subtype GMV differences across voxels between each pair of sites ($P < 0.05$, Bonferroni corrected). In addition, the GUANGZHOU site (first-episode cohort) had relatively low spatial similarity with the sites having chronic patients than those within chronic sites using either *K*-means ($r = [0.396:0.446]$ for GUANGZHOU vs. $[0.621:0.749]$ for chronic sites) or Hierarchical clustering method ($r = [0.471:0.568]$ for GUANGZHOU vs. $[0.589:0.822]$ for other sites) (Figures 2C and 3C).

Symptomatic features of the PANSS-derived subtypes

Mann–Whitney *U* test found PANSS-derived subtype-1 by *K*-means clustering had more severe symptoms in 28 of the 30 PANSS items (P1–4, 6–7; N1–7; G1–13, 15–16) than those of subtype-2 (Figure 4A). Similarly, PANSS-derived subtype-1 by Hierarchical

clustering had more severe symptoms in 26 of the 30 PANSS items (P1–3, 6–7; N1–7; G2–8, 10–16) than subtype-2 (Figure 4B). The inter-subtype PANSS difference pattern was replicated at each site (Figure 4C,D) ($P < 0.05$, Bonferroni corrected). Spatial Spearman correlation also demonstrated a significant positive association in *Z*-distributions of inter-subtype differences across PANSS items between each pair of sites ($P < 0.05$, Bonferroni corrected). In addition, the PANSS differences between symptomatic subtypes were more similar within Western (BrainGluSchi and COBRE, *K*-means: $r = 0.595$; Hierarchical: $r = 0.709$) or within Chinese cohorts (TIANJIN and GUANGZHOU, *K*-means: $r = 0.727$; Hierarchical: $r = 0.858$) than between races (*K*-means: $r = [0.371, 0.512]$; Hierarchical: $r = [0.482, 0.664]$) (Figure 4E,F).

PANSS differences between two GMV-derived subtypes

Mann–Whitney *U* test demonstrated no statistical differences in PANSS items scores between neuroanatomical subtypes based on *K*-means ($P > 0.05$, Bonferroni corrected), except that subtype-1 had a lower negative symptom (N4, passive/apathetic social withdrawal) than the subtype-2 (Figure 5A) ($P < 0.05$, Bonferroni corrected). Similarly, there were no statistical differences in any item of the PANSS scale between neuroanatomical subtypes based on the Hierarchical method (Figure 5B) ($P > 0.05$, Bonferroni corrected).

GMV difference between two PANSS-derived subtypes

Although both symptomatic subtypes had similar reduced GMV in the bilateral temporal cortex, hippocampus, MPFC, insula, and so on (Figure 5C–5D, left and middle panels) ($P < 0.05$, FWE corrected), there were no differences in GMV between the two symptomatic subtypes by either *K*-means (Figure 5C, right panel) or Hierarchical clustering (Figure 5D, right panel) ($P > 0.05$, FWE corrected).

Similarity between GMV- and PANSS-derived subtypes

Cohen's Kappa test was employed to explore the similarity of subtyping results between different subtyping features (GMV vs. PANSS), or between different subtyping methods (*K*-means vs. Hierarchical). A very low Kappa score was found between the neuroanatomical subtypes and symptomatic subtypes either by *K*-means (Kappa = 0.004, $P = 0.946$) (Figure 6A), or Hierarchical clustering (Kappa = -0.051, $P = 0.356$) (Figure 6B). In contrast, a high Kappa score was found between the neuroanatomical subtypes by *K*-means and those by Hierarchical clustering (Kappa = 0.596, $P < 0.001$) (Figure 6C), and between the symptomatic subtypes by *K*-means and those by Hierarchical clustering (Kappa = 0.754, $P < 0.001$) (Figure 6D). The dissimilarity pattern between GMV-derived subtypes and PANSS-derived subtypes could be replicated in each site (Supplementary Figures 1–4).

Discussion

In this study, we applied unsupervised ML methods to subtype schizophrenia patients into two neuroanatomical and two symptomatic subtypes, respectively. We found no differences in GMV between the PANSS-derived symptomatic subtypes and almost no differences in PANSS scores between the GMV-derived neuroanatomical subtypes. Moreover, the GMV-derived and PANSS-derived subtypes are mismatched in patients belonging. The

Table 2. Demographic and clinical characteristics of the schizophrenia subtypes and healthy controls

Method and metrics	Demos	Subtype-1	Subtype-2	Healthy controls	Statistics	P-value
K-means based on GMV data	Number of subjects	182	132	257	–	–
	Age	33.58 ± 10.81	34.12 ± 11.34	34.40 ± 10.91	0.299 ^a	0.742
	Male/Female	130/52	87/45	159/98	4.331 ^b	0.117
	TIV	1497.01 ± 163.08	1487.83 ± 179.94	1494.35 ± 146.55	0.130 ^a	0.878
	Total CPZ	300 (150, 500)	400 (262.5, 600)	–	–2.859 ^c	0.004*
	Age when schizophrenia was first diagnosed	19.5 (17, 25)	21 (17.75, 26)	–	–1.194 ^c	0.232
	Age when symptoms first appeared	19 (16.25, 24)	20 (17, 25)	–	–1.865 ^c	0.062
	Age when therapy was first received	20 (17, 26)	22 (18, 28)	–	–1.836 ^c	0.066
	Ill duration	11 (5.75, 19)	9 (5, 16.25)	–	–1.350 ^c	0.177
	Education level	4 (3, 5)	4 (3, 5)	–	–0.352 ^c	0.725
K-means based on PANSS scores	Number of subjects	122	192	257	–	–
	Age	34.03 ± 11.06	33.66 ± 11.04	34.40 ± 10.91	0.247 ^a	0.781
	Male/Female	80/42	137/55	159/98	4.403 ^b	0.110
	TIV	1486.04 ± 164.50	1497.67 ± 173.92	1494.35 ± 146.55	0.201 ^a	0.818
	Total CPZ	400 (240, 600)	300 (167, 565)	–	–1.293 ^c	0.196
	Age when schizophrenia was first diagnosed	20 (17, 25.75)	21 (18, 25)	–	–0.254 ^c	0.800
	Age when symptoms first appeared	19 (17, 24.75)	19.5 (17, 24.25)	–	–0.477 ^c	0.633
	Age when therapy was first received	21 (18, 27)	21 (18, 27)	–	–0.279 ^c	0.780
	Ill duration	9 (4, 20)	10 (6, 18)	–	–0.152 ^c	0.879
	Education level	4 (3, 5)	4 (3, 5)	–	–0.530 ^c	0.596
Hierarchical based on GMV data	Number	116	198	257	–	–
	Age	32.75 ± 10.61	34.42 ± 11.24	34.40 ± 10.91	1.057 ^a	0.348
	Male/Female	84/32	133/65	159/98	4.189 ^b	0.125
	TIV	1505.76 ± 175.10	1485.76 ± 167.19	1494.35 ± 146.55	0.575 ^a	0.563
	Total CPZ	240 (100, 500)	400 (225, 600)	–	–3.007 ^c	0.003*
	Age when schizophrenia was first diagnosed	19 (17, 23)	21 (18, 27)	–	–2.064 ^c	0.039*
	Age when symptoms first appeared	18 (17, 22)	20 (17, 25.5)	–	–1.998 ^c	0.046*
	Age when therapy was first received	19 (17, 24.5)	22 (18, 28.25)	–	–2.994 ^c	0.003*
	Ill duration	11 (6.25, 19)	9 (5, 17.5)	–	–1.131 ^c	0.259
	Education level	3 (3, 5)	4 (3, 5)	–	–0.939 ^c	0.348
Hierarchical based on PANSS scores	Number	146	168	257	–	–
	Age	33.94 ± 11.17	33.69 ± 10.94	34.40 ± 10.91	0.225 ^a	0.799
	Male/Female	97/49	120/48	159/98	4.160 ^b	0.127
	TIV	1492.06 ± 166.76	1494.10 ± 173.54	1494.35 ± 146.55	0.010 ^a	0.990
	Total CPZ	375 (240, 600)	300 (150, 600)	–	–0.966 ^c	0.334
	Age when schizophrenia was first diagnosed	20 (17, 25)	21 (18, 26)	–	–0.971 ^c	0.332
	Age when symptoms first appeared	19 (17, 24)	20 (17, 25)	–	–0.618 ^c	0.537
	Age when therapy was first received	20 (18, 25)	22 (18, 28)	–	–0.708 ^c	0.479
	Ill duration	11 (5, 20)	10 (5, 17)	–	–0.729 ^c	0.466
	Education level	4 (3, 5)	4 (3, 5)	–	–0.891 ^c	0.373

^aANOVA.^bChi-square test.^cMann–Whitney *U* test.

*represent statistically significant items.

Kmeans clustering based on GMV

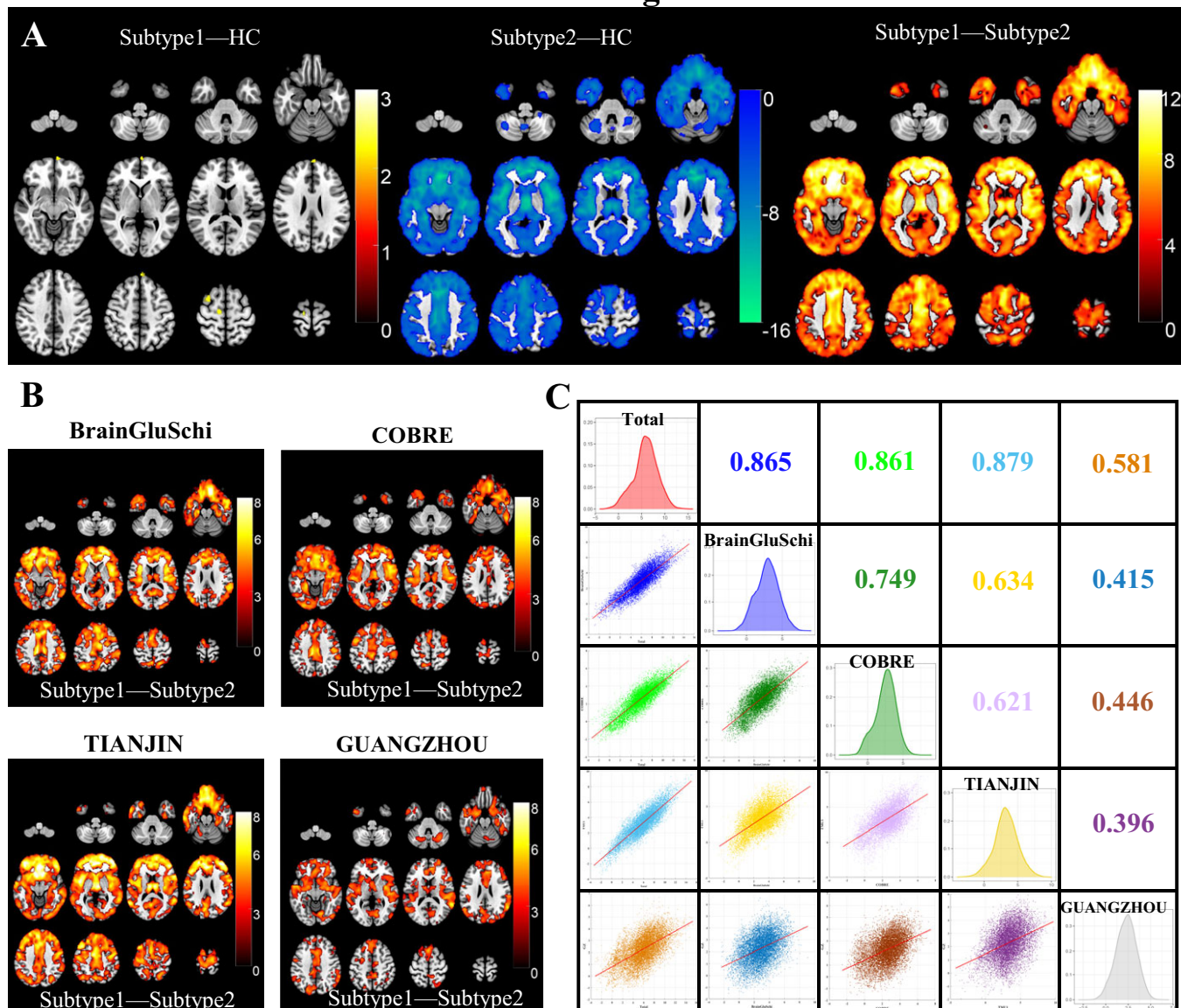


Figure 2. Schizophrenia neuroanatomical subtypes based on *K*-means clustering. (A) Intergroup differences in GMV between schizophrenia neuroanatomical subtypes by *K*-means clustering and HCs. (B) Inter-subtype differences in GMV at each site. The color bar represents the *T* values. (C) The Spearman spatial correlation in *T* values of inter-subtype GMV differences between each pair of sites.

dissociation patterns were replicated in four independent sites with different disease progressions (chronic vs. first episodes) and different ancestors (Chinese vs. Western) and were validated by different clustering methods (*K*-means vs. Hierarchical). To our knowledge, this is the first study directly reporting the dissociations between ML-based neuroanatomical subtypes and ML-based symptomatic subtypes of schizophrenia. These findings may provide a new viewpoint toward understanding the heterogeneity of schizophrenia.

One of the most important findings is that we found two replicable ML-based neuroanatomical subtypes, with one showing broadly reduced GMV and the other having focally increased GMV, but almost no differences in PANSS item scores between the two GMV-based neuroanatomical subtypes. These findings were consistent with early studies showing no PANSS differences between neuroimaging subtypes using GMV by several independent studies [5, 12, 13, 27, 31]. Our findings seem inconsistent with

one study by Gupta et al. [30], who categorized schizophrenia into three subtypes (S_1 , S_2 , and S_{inter}) by manually setting a loading cutoff (mean \pm std) for two independent components derived from source-based morphometry. Although they found a statistical difference in positive symptoms between the S_1 and S_2 , this subtyping method is not strictly ascribed to “unsupervised” ML, and the comparison ignored a large subset with an intermediate state. Another study reported only differences in negative symptoms between neuroimaging subtypes derived from white matter DTI metrics [26]. In this study, we excluded the possible influences of clustering methods and sites on ML-based subtyping, suggesting that the absence of PANSS differences between ML-based GMV subtypes is reliable.

We also identified two ML-based symptomatic subtypes, with one having generally more severe PANSS symptoms than the other, but the two ML-based symptomatic subtypes showed no statistical differences in GMV. In supporting our findings, although brain

Hierarchical clustering based on GMV

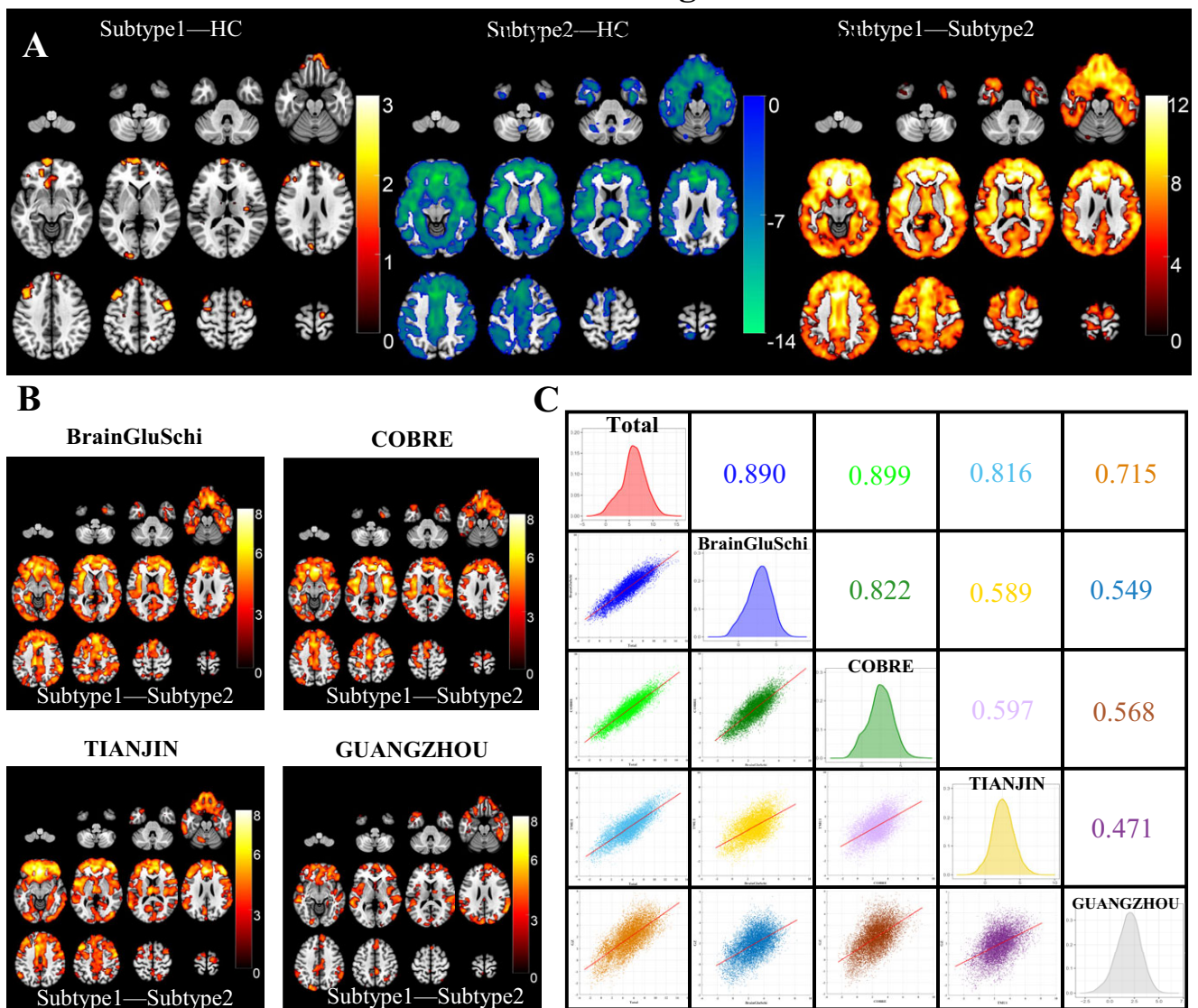


Figure 3. Schizophrenia neuroanatomical subtypes based on Hierarchical clustering. (A) Intergroup differences in GMV between schizophrenia neuroanatomical subtypes by Hierarchical clustering and HCs. (B) Inter-subtype differences in GMV at each site. The color bar represents the *T* values. (C) Spearman spatial correlation in *T* values of inter-subtype GMV differences between each pair of sites.

structural differences were reported among PANSS-based symptomatic subtypes based on some multivariate pattern analyses, most studies only reported subtle differences, no difference, or considerable overlap in brain signatures among symptomatic subtypes [16, 17, 19, 20, 36]. It should be noted that early studies have reported cerebral structural alterations associated with symptoms of psychosis, such as auditory verbal hallucinations (AVH) [37, 38], which seems to contradict the present findings. However, a meta-analysis did not find any GMV difference between patients with AVH and those without AVH, but a significant association between the severity of AVH and GMV reduction in the superior temporal gyri [39]. Similar to the meta-analysis, our study did not find a statistical difference in hallucination symptoms (P3 item of PANSS) between the two schizophrenia anatomical subtypes. The possible explanation for inconsistent AVH-related GMV changes included: First, AVH is a state characteristic that changes dynamically with disease course [38]. Second, psychometric

heterogeneities and/or different AVH subtypes (episodic, persistent symptoms, and treatment-resistant) may exist across studies [39]. Finally, long-term antipsychotics can suppress AVH symptoms and affect brain atrophy, complicating the associations between brain damage and AVH [40, 41].

Multiple factors may explain the dissociation between neuroanatomical subtyping and symptomatic subtyping. First, the classification of symptomatic subtypes may be affected by: (1) Dimension overlap. The symptom diversity might also be accompanied by overlapping and coexisting symptom dimensions, which may cause difficulty in determining subtypes. (2) Comorbidity and shared symptoms across psychiatric diseases [42]. It has been reported that some psychotic diseases, such as bipolar disorder and major depressive disorder, may be misdiagnosed as schizophrenia because of their shared symptoms or clinical features [43, 44]. (3) Symptom dynamics during disease progression. The patients with positive symptoms became progressively less

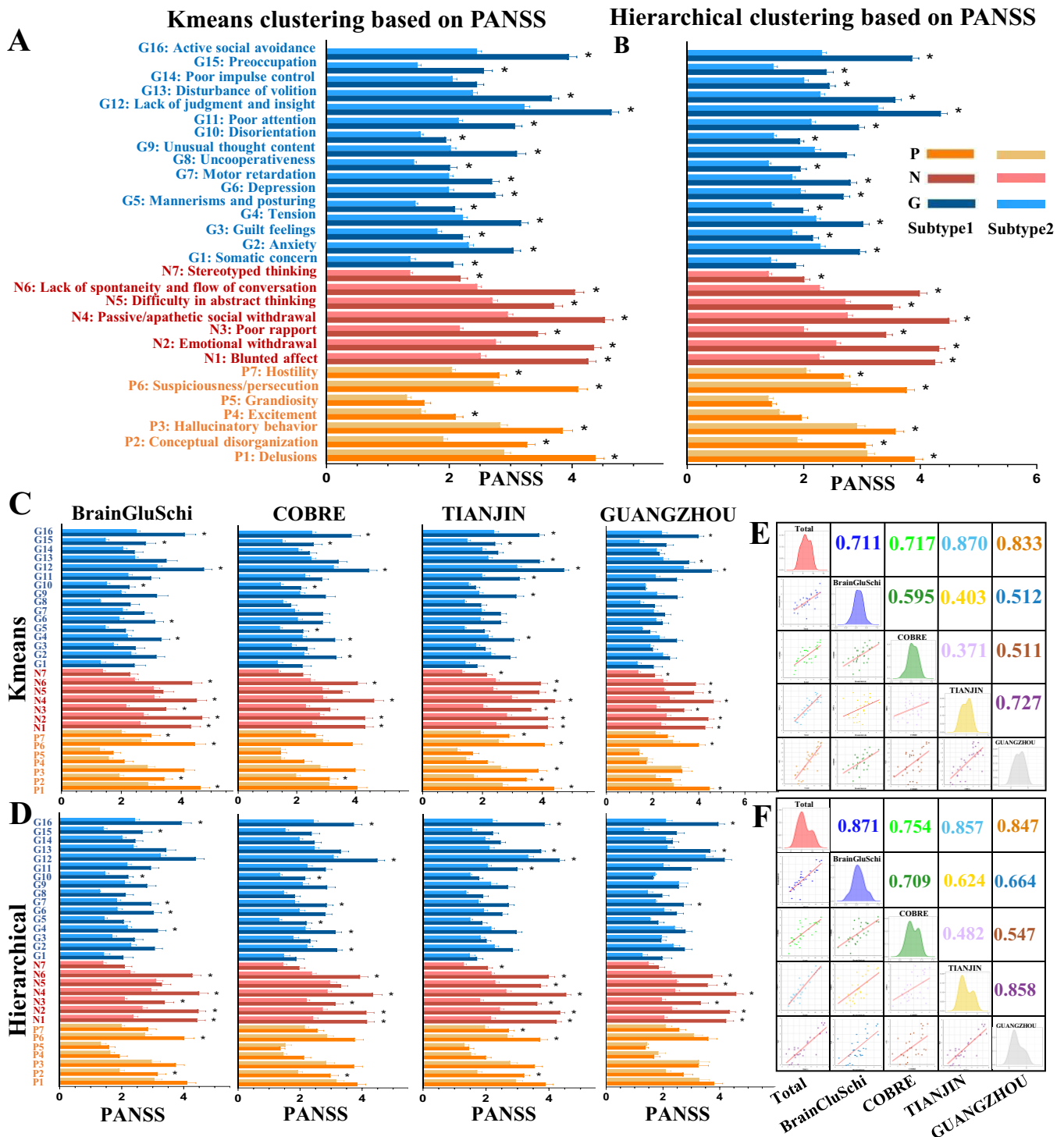


Figure 4. Schizophrenia symptomatic subtypes based on *K*-means and Hierarchical clustering. (A) Inter-subtype differences in PANSS scores clustered by *K*-means algorithm. (B) Inter-subtype differences in PANSS scores clustered by Hierarchical algorithm. (C) Inter-subtype differences in PANSS scores for each site clustered by *K*-means algorithm. (D) Inter-subtype differences in PANSS scores for each site clustered by Hierarchical algorithm. (E) Spearman correlation in *T* values of inter-subtype PANSS differences between each pair of sites by *K*-means algorithm. (F) Spearman correlation in *T* values of inter-subtype PANSS differences between each pair of sites by Hierarchical algorithm.

conspicuous and were gradually replaced with negative and disorganized phenotypes [45, 46]. Second, regarding neuroanatomical subtyping classification, early studies had reported that Olanzapine could lead to GMV loss after 1 year's treatment [47], while risperidone and ziprasidone could partially reverse brain atrophy

[48]. All these neuroanatomical and symptomatic subtyping uncertainties could cause mismatches between neuroanatomical and symptomatic subtypes. Finally, the mismatch in the time course between GMV changes and symptoms may also cause subtyping dissociation. For example, early studies have revealed that GMV

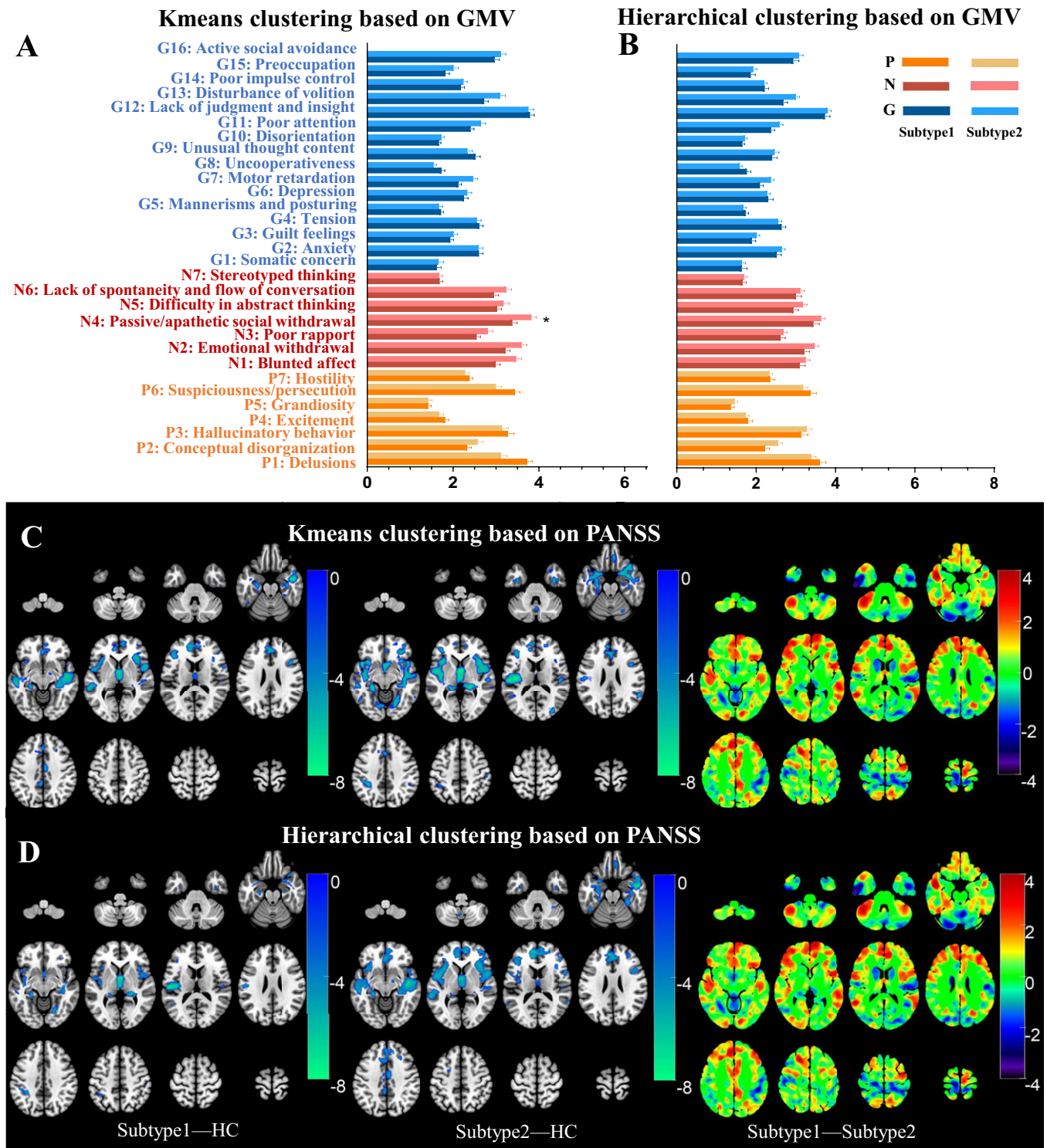


Figure 5. Dissociated GMV- and PANSS-derived subtypes as identified by inter-subtype comparisons. (A) PANSS differences between two GMV-derived subtypes by *K*-means algorithm. (B) PANSS differences between two GMV-derived subtypes by Hierarchical algorithm. (C) GMV differences between two PANSS-derived subtypes by *K*-means algorithm did not survived after FWE correction. (D) GMV differences between two PANSS-derived subtypes by Hierarchical algorithm did not survived after FWE correction.

changes have occurred in prodromal or even symptom-free individuals, which are not matched with their symptoms [19, 49, 50].

In our study, the GMV changes between neuroanatomical subtypes were relatively broader in chronic schizophrenia patients (BrainGluSchi, COBRE, TIANJIN) than the first-episode drug-

naïve ones (GUANGZHOU). We also found that the CPZ equivalent of neuroanatomical subtype 2 (widespread GMV loss) was higher than that of neuroanatomical subtype 1 (focal GMV increase). Previous *in vivo* and *ex vivo* MRI and postmortem histological studies suggested that exposure to antipsychotic

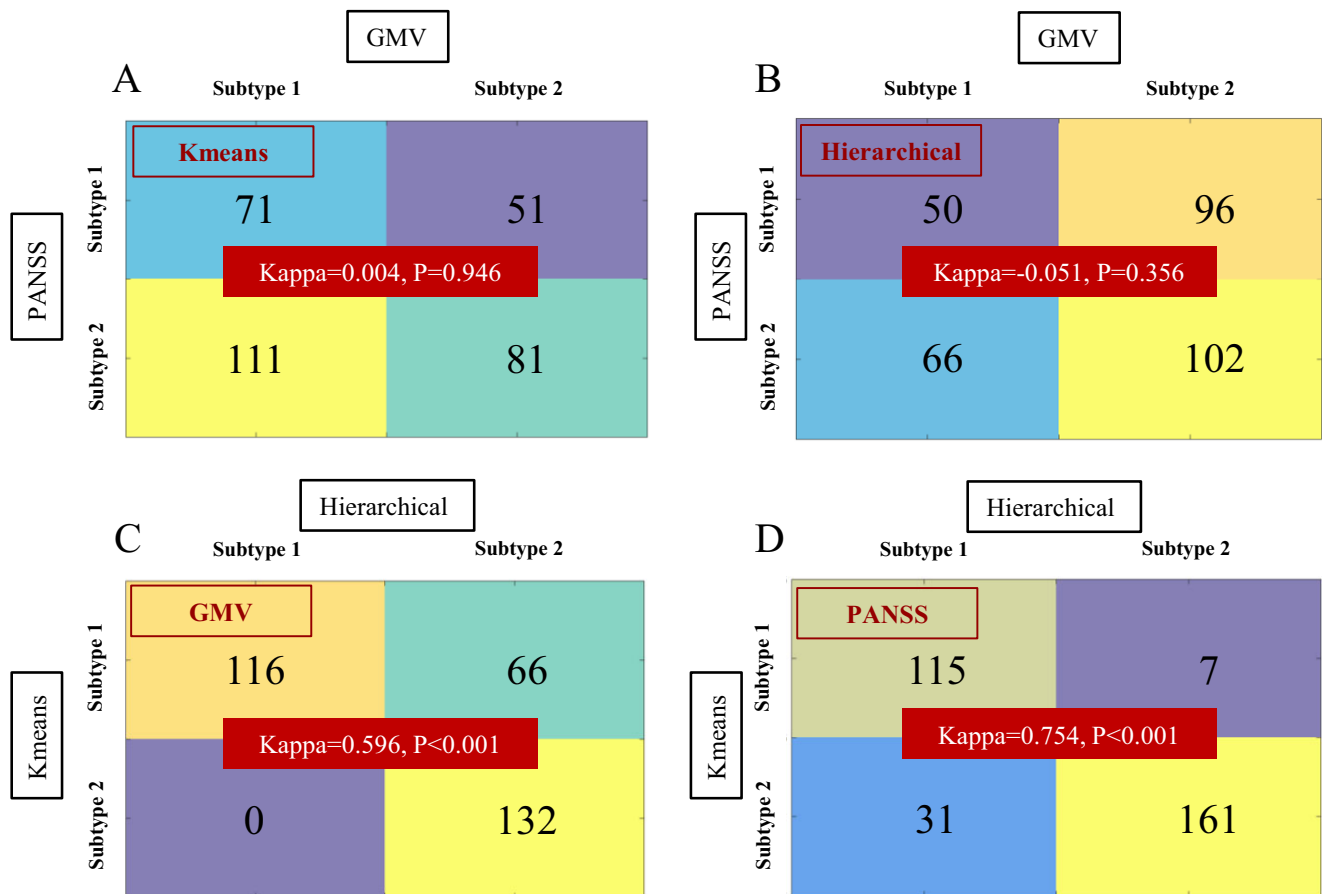


Figure 6. Subtypes consistency comparisons between different features and between different clustering methods. A Kappa test was employed to explore the consistency of subtypes using different subtyping features (GMV vs. PANSS) or between different subtyping methods (*K*-means vs. Hierarchical). (A) GMV versus PANSS subtypes consistency using *K*-means clustering; (B) GMV versus PANSS subtypes consistency using Hierarchical clustering; (C) GMV subtypes consistency between *K*-means and Hierarchical clustering methods; (D) PANSS subtypes consistency between *K*-means and Hierarchical clustering methods.

treatment causes significantly reduced whole brain volume, especially gray matter [51–53]. Thus, antipsychotic drugs could partially explain the wider brain atrophy in neuroanatomical subtype-2 chronic patients [54]. It should be noted that the slight difference in subtypes between chronic and first-episode datasets was not evident for PANSS-based symptomatic subtypes. Instead, we found PANSS differences between symptomatic subtypes were more similar within Western (BrainGluSchi and COBRE) or within Chinese cohorts (TIANJIN and GUANGZHOU) than between them, which may be caused by heterogeneities in psychiatrists' evaluations of PANSS and patients recruitments between the Western and Chinese cohorts.

Although we did not find any symptomatic differences between the ML-based neuroanatomical subtypes, the potential clinical meanings of our findings included: (1) Neuroanatomical subtypes could deepen our understanding of the biological heterogeneity of internal traits of schizophrenia. Compared to the symptomatic subtypes, the neuroanatomical subtypes were relatively stable and varied to a lesser over time than clinical symptoms [30], and thus may more closely represent the biological heterogeneity. For example, neuroanatomic subtypes were reported to be closely associated with brain tissue expression heterogeneities of schizophrenia risk genes [55]. One recent study also reported distinctive cortical damage patterns between subtypes with and without prominent alterations in methylation and immune features

[52]. (2) Neuroanatomical subtypes may increase the diagnosis accuracy by resolving the inter-patient heterogeneities. It has been shown that the subtyping improved the computer-aided diagnostic accuracy of schizophrenia patients from control subjects using neuroanatomical measures [12]. (3) Neuroanatomical subtypes may predict therapeutic outcomes. This study found two neuroanatomical subtypes: one with focally increased GMV and the other with broadly reduced GMV, similar to Chand's findings [5]. Early neuroanatomic studies suggest that patients with more GMV reduction are marked with relatively poor outcomes [56]. The regions with increased GMV in subtype 1 were supposed to be related to the dopaminergic system [57], while the broad GMV decreases in subtype 2 may be associated with the glutamatergic and GABAergic systems [58]. Thus, the neuroanatomical subtypes may be sensitive to drugs acting on different pathways, which should be validated in the future.

Our studies have some limitations. First, although the dissociation patterns between the schizophrenia neuroanatomical and symptomatic subtypes were validated in four independent sites with different disease progressions and ancestors by different clustering methods, this study is a cross-sectional design, and the number of enrolled sites is relatively small. Thus, future longitudinal studies with more involved sites are preferred to validate our hypothesis. Second, we only introduced GMV for subtyping. Other neuroimaging techniques, such as diffusion MRI and functional

MRI, would provide additional knowledge about the heterogeneity of schizophrenia. As a result, it is hoped to combine multimodal neuroimaging features to recognize schizophrenia subtypes to more fully characterize the biological heterogeneities of schizophrenia. Finally, we have not directly associated the identified subtypes with underlying neurobiological basis, including their association with genetic, epigenetic, transcriptomic, metabolic, and treatment heterogeneities. This issue is critical for understanding the neurobiological underpinnings of heterogeneity and contributing to precision medicine.

Supplementary Material. The supplementary material for this article can be found at <http://doi.org/10.1192/j.eurpsy.2023.2446>.

Data availability statement. The critical data and scripts for clustering analyses were publicly available on the website (https://github.com/BrainWanderLab/Schizophrenia_subtyping_GMV_PANSS).

Author contribution. C.Y. and W.Q. contributed to the concept and design of the study. C.Z., B.Z., Y.N., and W.Q. contributed to the data acquisition. C.C., H.D., X.D., Y.X., W.M., Y.Z., Y.J., M.L., and W.Q. contributed to the data analysis. C.C. and W.Q. contributed to the drafting of the manuscript. C.Y. and W.Q. contributed to the supervision and critical revision of the manuscript. All authors approved the final version to be submitted.

Financial support. This work was supported by the National Natural Science Foundation of China (grant numbers 81971599 and 81771818 for W.Q., 82030053 for C.Y., and 81971694 for M.L.); National Key Research and Development Program of China (grant number 2018YFC1314300 for C.Y.); Tianjin Natural Science Foundation (grant number 19JCYBJC25100 for W.Q. and 21JCQNJC01480 for C.C.); Tianjin Health High Level Talent Selection and Training Project (grant number TJSQNYXXR-D2-143 for C.C.); and Tianjin Health Research Project (grant number TJWJ2023QN031 for C.C.).

Competing interest. The authors declare no conflict of interest.

References

- Millan MJ, Andrieux A, Bartzokis G, Cadenhead K, Dazzan P, Fusar-Poli P, et al. Altering the course of schizophrenia: progress and perspectives. *Nat Rev Drug Discov.* 2016;15:485–515.
- Owen MJ, Sawa A, Mortensen PB. Schizophrenia. *Lancet.* 2016;388:86–97.
- McCutcheon RA, Reis Marques T, Howes OD. Schizophrenia – an overview. *JAMA Psychiatry.* 2020;77:201–10.
- Hjorthøj C, Stürup AE, McGrath JJ, Nordentoft M. Years of potential life lost and life expectancy in schizophrenia: a systematic review and meta-analysis. *Lancet Psychiatry.* 2017;4:295–301.
- Chand GB, Dwyer DB, Erus G, Sotiras A, Varol E, Srinivasan D, et al. Two distinct neuroanatomical subtypes of schizophrenia revealed using machine learning. *Brain.* 2020;143:1027–38.
- Di Biase MA, Geaghan MP, Reay WR, Seidlitz J, Weickert CS, Pebay A, et al. Cell type-specific manifestations of cortical thickness heterogeneity in schizophrenia. *Mol Psychiatry.* 2022;27:2052–60.
- Wen J, Varol E, Sotiras A, Yang Z, Chand GB, Erus G, et al. Multi-scale semi-supervised clustering of brain images: deriving disease subtypes. *Med Image Anal.* 2022;75:102304.
- Liang S, Wang Q, Greenshaw AJ, Li X, Deng W, Ren H, et al. Aberrant triple-network connectivity patterns discriminate biotypes of first-episode medication-naïve schizophrenia in two large independent cohorts. *Neuropsychopharmacology.* 2021;46:1502–9.
- Yamashita A, Yahata N, Itahashi T, Lisi G, Yamada T, Ichikawa N, et al. Harmonization of resting-state functional MRI data across multiple imaging sites via the separation of site differences into sampling bias and measurement bias. *PLoS Biol.* 2019;17:e3000042.
- Mizuno Y, McCutcheon RA, Brugger SP, Howes OD. Heterogeneity and efficacy of antipsychotic treatment for schizophrenia with or without treatment resistance: a meta-analysis. *Neuropsychopharmacology.* 2020;45:622–31.
- McCutcheon RA, Pillinger T, Mizuno Y, Montgomery A, Pandian H, Vano L, et al. The efficacy and heterogeneity of antipsychotic response in schizophrenia: A meta-analysis. *Mol Psychiatry.* 2021;26:1310–20.
- Dwyer DB, Cabral C, Kameitz-Illankovic L, Sanfelici R, Kameitz J, Calhoun V, et al. Brain subtyping enhances the neuroanatomical discrimination of schizophrenia. *Schizophr Bull.* 2018;44:1060–9.
- Xiao Y, Liao W, Long Z, Tao B, Zhao Q, Luo C, et al. Subtyping schizophrenia patients based on patterns of structural brain alterations. *Schizophr Bull.* 2022;48:241–50.
- Braff DL, Ryan J, Rissling AJ, Carpenter WT. Lack of use in the literature from the last 20 years supports dropping traditional schizophrenia subtypes from DSM-5 and ICD-11. *Schizophr Bull.* 2013;39:751–3.
- Kay SR, Fiszbein A, Opler LA. The Positive and Negative Syndrome Scale (PANSS) for schizophrenia. *Schizophr Bull.* 1987;13:261–76.
- Zhang T, Koutsouleris N, Meisenzahl E, Davatzikos C. Heterogeneity of structural brain changes in subtypes of schizophrenia revealed using magnetic resonance imaging pattern analysis. *Schizophr Bull.* 2015;41:74–84.
- Koutsouleris N, Gaser C, Jager M, Bottlender R, Frodl T, Holzinger S, et al. Structural correlates of psychopathological symptom dimensions in schizophrenia: a voxel-based morphometric study. *NeuroImage.* 2008;39:1600–12.
- Chen J, Patil KR, Weis S, Sim K, Nickl-Jockschat T, Zhou J, et al. Neurobiological divergence of the positive and negative schizophrenia subtypes identified on a new factor structure of psychopathology using non-negative factorization: an international machine learning study. *Biol Psychiatry.* 2020;87:282–93.
- Nenadic I, Sauer H, Gaser C. Distinct pattern of brain structural deficits in subtypes of schizophrenia delineated by psychopathology. *NeuroImage.* 2010;49:1153–60.
- Nenadic I, Yotter RA, Sauer H, Gaser C. Patterns of cortical thinning in different subgroups of schizophrenia. *Br J Psychiatry.* 2015;206:479–83.
- Lim K, Smucny J, Barch DM, Lam M, Keefe RSE, Lee J. Cognitive subtyping in schizophrenia: a latent profile analysis. *Schizophr Bull.* 2021;47:712–21.
- Watson AJ, Giordano A, Suckling J, Barnes TRE, Husain N, Jones PB, et al. Cognitive function in early-phase schizophrenia-spectrum disorder: IQ subtypes, brain volume and immune markers. *Psychol Med.* 2022;1–10.
- Lewandowski KE. Genetically, developmentally, and clinically distinct cognitive subtypes in schizophrenia: a tale of three trajectories. *Am J Psychiatry.* 2020;177:282–4.
- Pelin H, Ising M, Stein F, Meinert S, Meller T, Brosch K, et al. Identification of transdiagnostic psychiatric disorder subtypes using unsupervised learning. *Neuropsychopharmacology.* 2021;46:1895–905.
- Jordan MI, Mitchell TM. Machine learning: trends, perspectives, and prospects. *Science.* 2015;349:255–60.
- Sun H, Lui S, Yao L, Deng W, Xiao Y, Zhang W, et al. Two patterns of white matter abnormalities in medication-naïve patients with first-episode schizophrenia revealed by diffusion tensor imaging and cluster analysis. *JAMA Psychiatry.* 2015;72:678–86.
- Honnorat N, Dong A, Meisenzahl-Lechner E, Koutsouleris N, Davatzikos C. Neuroanatomical heterogeneity of schizophrenia revealed by semi-supervised machine learning methods. *Schizophr Res.* 2019;214:43–50.
- Rozycki M, Satterthwaite TD, Koutsouleris N, Erus G, Doshi J, Wolf DH, et al. Multisite machine learning analysis provides a robust structural imaging signature of schizophrenia detectable across diverse patient populations and within individuals. *Schizophr Bull.* 2018;44:1035–44.
- Ma L, Rolls ET, Liu X, Liu Y, Jiao Z, Wang Y, et al. Multi-scale analysis of schizophrenia risk genes, brain structure, and clinical symptoms reveals integrative clues for subtyping schizophrenia patients. *J Mol Cell Biol.* 2019;11:678–87.
- Gupta CN, Castro E, Rachkonda S, van Erp TGM, Potkin S, Ford JM, et al. Biclustered independent component analysis for complex biomarker and subtype identification from structural magnetic resonance images in schizophrenia. *Front Psych.* 2017;8:179.

- [31] Zhao Q, Cao H, Zhang W, Li S, Xiao Y, Tamminga CA, et al. A subtype of institutionalized patients with schizophrenia characterized by pronounced subcortical and cognitive deficits. *Neuropsychopharmacology*. 2022;47:2024–32.
- [32] Drysdale AT, Grosenick L, Downar J, Dunlop K, Mansouri F, Meng Y, et al. Resting-state connectivity biomarkers define neurophysiological subtypes of depression. *Nat Med*. 2017;23:28–38.
- [33] Wang L, Alpert KI, Calhoun VD, Cobia DJ, Keator DB, King MD, et al. SchizConnect: mediating neuroimaging databases on schizophrenia and related disorders for large-scale integration. *NeuroImage*. 2016;124:1155–67.
- [34] Landis D, Courtney W, Dieringer C, Kelly R, King M, Miller B, et al. COINS data exchange: an open platform for compiling, curating, and disseminating neuroimaging data. *NeuroImage*. 2016;124:1084–8.
- [35] Fortin JP, Cullen N, Sheline YI, Taylor WD, Aselcioglu I, Cook PA, et al. Harmonization of cortical thickness measurements across scanners and sites. *NeuroImage*. 2018;167:104–20.
- [36] Sallet PC EH, Alves TM, Oliveira JR, Sassi E, Campi de Castro C, Busatto GF, et al. Reduced cortical folding in schizophrenia – an MRI morphometric study. *Am J Psychiatry*. 2003;160:1606–13.
- [37] Di Biase MA, Zhang F, Lyall A, Kubicki M, Mandl RCW, Sommer IE, et al. Neuroimaging auditory verbal hallucinations in schizophrenia patient and healthy populations. *Psychol Med*. 2020;50:403–12.
- [38] Kubera KM, Sambataro F, Vasic N, Wolf ND, Frasch K, Hirjak D, et al. Source-based morphometry of gray matter volume in patients with schizophrenia who have persistent auditory verbal hallucinations. *Prog Neuro-Psychopharmacol Biol Psychiatry*. 2014;50:102–9.
- [39] Modinos G, Costafreda SG, van Tol MJ, McGuire PK, Aleman A, Allen P. Neuroanatomy of auditory verbal hallucinations in schizophrenia: a quantitative meta-analysis of voxel-based morphometry studies. *Cortex*. 2013;49:1046–55.
- [40] Di Biase MA, Croypley VL, Baune BT, Olver J, Amminger GP, Phassouliotis C, et al. White matter connectivity disruptions in early and chronic schizophrenia. *Psychol Med*. 2017;47:2797–810.
- [41] Di Biase MA, Croypley VL, Cocchi L, Fornito A, Calamante F, Ganella EP, et al. Linking cortical and connective pathology in schizophrenia. *Schizophr Bull*. 2019;45:911–23.
- [42] Chang M, Womer FY, Gong X, Chen X, Tang L, Feng R, et al. Identifying and validating subtypes within major psychiatric disorders based on frontal-posterior functional imbalance via deep learning. *Mol Psychiatry*. 2021;26:2991–3002.
- [43] Harris MA, Shen X, Cox SR, Gibson J, Adams MJ, Clarke TK, et al. Stratifying major depressive disorder by polygenic risk for schizophrenia in relation to structural brain measures. *Psychol Med*. 2020;50:1653–62.
- [44] Van Rheenen TE, Lewandowski KE, Tan EJ, Ospina LH, Ongur D, Neill E, et al. Characterizing cognitive heterogeneity on the schizophrenia-bipolar disorder spectrum. *Psychol Med*. 2017;47:1848–64.
- [45] McGlashan TH. The profiles of clinical deterioration in schizophrenia. *J Psychiatr Res*. 1998;32:133–41.
- [46] Wang Z, Xue Z, Pu W, Yang B, Li L, Yi W, et al. Comparison of first-episode and chronic patients diagnosed with schizophrenia: symptoms and childhood trauma. *Early Interv Psychiatry*. 2013;7:23–30.
- [47] Lieberman TG, Charles C, Zipursky R, Sharma T, Kahn RS, Keefe RS, et al. Antipsychotic drug effects on brain morphology in first-episode psychosis. *Arch Gen Psychiatry*. 2015;20:84–97.
- [48] Garver DL, Holcomb JA, Christensen JD. Cerebral cortical gray expansion associated with two second-generation antipsychotics. *Biol Psychiatry*. 2005;58:62–6.
- [49] Shan XX, Ou YP, Pan P, Ding YD, Zhao J, Liu F, et al. Increased frontal gray matter volume in individuals with prodromal psychosis. *CNS Neurosci Ther*. 2019;25:987–94.
- [50] Buechler R, Wotruba D, Michels L, Theodoridou A, Metzler S, Walitza S, et al. Cortical volume differences in subjects at risk for psychosis are driven by surface area. *Schizophr Bull*. 2020;46:1511–9.
- [51] Vernon AC, Natesan S, Modo M, Kapur S. Effect of chronic antipsychotic treatment on brain structure: a serial magnetic resonance imaging study with ex vivo and postmortem confirmation. *Biol Psychiatry*. 2011;69:936–44.
- [52] Luo C, Pi X, Hu N, Wang X, Xiao Y, Li S, et al. Subtypes of schizophrenia identified by multi-omic measures associated with dysregulated immune function. *Mol Psychiatry*. 2021;26:6926–36.
- [53] Liang L, Silva AM, Jeon P, Ford SD, MacKinley M, Theberge J, et al. Widespread cortical thinning, excessive glutamate and impaired linguistic functioning in schizophrenia: a cluster analytic approach. *Front Hum Neurosci*. 2022;16:954898.
- [54] Cahn HPH, Lems EB, van Haren NE, Schnack HG, van der Linden JA, Schothorst PF, van Engeland H, Kahn RS. Brain volume changes in first-episode schizophrenia. *Arch Gen Psychiatry*. 2002;59:1002–10.
- [55] Ji Y, Zhang X, Wang Z, Qin W, Liu H, Xue K, et al. Genes associated with gray matter volume alterations in schizophrenia. *NeuroImage*. 2021;225:117526.
- [56] McGuire P, Dazzan PJWP. Does neuroimaging have a role in predicting outcomes in psychosis? *World Psychiatry* 2017;16:209.
- [57] Cannon TD. How schizophrenia develops: cognitive and brain mechanisms underlying onset of psychosis. *Trends Cogn Sci*. 2015;19:744–56.
- [58] Howes O, McCutcheon R, Stone J. Glutamate and dopamine in schizophrenia: an update for the 21st century. *J Psychopharmacol*. 2015;29:97–115.